Simulated Body Fluids Prepared with Natural Buffers and System for Active pH Regulation

Gligorijević, Bojan Rade*[+]

University of Belgrade, Innovation Centre of Faculty of Technology and Metallurgy, Karnegijeva 4,
11120 Belgrade, SERBIA

Vilotijević, Miroljub Novak

University of Belgrade, Vinča Institute of Nuclear Sciences, Mike Petrovića Alasa 12-14, 11001 Belgrade,
Serbia and Plasma Jet Co, Braničevska 29, 11000 Belgrade, SERBIA

ABSTRACT: *The current study focuses on creating an initial highly alkaline simulated body fluid whose pH can be decreased to a physiological range by adding CO_2 (protein-free simulated body fluid) or a combination of CO_2 and human proteins (protein-containing simulated body fluid). The effects of dissolved human proteins, Ca^{2+} ions, and immersed plasma-sprayed hydroxyapatite coatings on the pH and chemical instability of prepared simulated body fluids were investigated. The physiological concentration of dissolved human proteins decreased the pH instability in prepared simulated body fluids by 60% and the physiological concentration of dissolved Ca^{2+} ions by 15%. The effect of immersing the hydroxyapatite coatings was negligible. In terms of chemical instability, the dissolution of Ca^{2+} ions caused the blurring of protein-free simulated body fluids after 0.6-1.0 h. In protein-containing simulated body fluids, this phenomenon was undetectable due to their opacity. The effects of human protein presence on the carbonated-apatite-forming ability on the surfaces of immersed hydroxyapatite coatings in the prepared simulated body fluids were also assessed. The experiments validated the bioactivity of plasma-sprayed hydroxyapatite coatings in the prepared simulated body fluids, regardless of protein presence. On the other hand, under the different experimental conditions (unregulated or regulated pH), the human protein presence had an inhibitory (unregulated pH) or indifferent/promoting (regulated pH) influence on the carbonated-apatite-forming ability. The results of the present study are discussed, as well as the strengths and shortcomings of the prepared simulated body fluids, and are compared to those of previous relevant investigations.*

KEYWORDS: *Simulated body fluid; Human proteins; Hydroxyapatite coatings; pH stability; Carbonated apatite formation.*

INTRODUCTION

Up until 1990s, many different physiological solutions were developed to simulate the composition of the human blood plasma [1-12]. In 1990, *Kokubo et al.* created "conventional simulated body fluid" (con-SBF) [7,13], which has since become the standard SBF for in-vitro testing of model implants (ISO 23317). In order to improve

the accuracy of the con-SBF composition, extensive research on the subject was continued [14-17]. Finally, in 2002-2003, *Oyane et al.* made progress in SBF development by reporting the „revised simulated body fluid" (r-SBF) with the exact composition of the inorganic part of the normal human blood plasma [18,19]. However, the r-SBF was a highly pH and chemically unstable electrolyte solution because it contained a high HCO_3^- concentration of 27 mmol/L [18,19]. For this reason, *Oyane et al.* proposed a more stable „modified simulated body fluid " (m-SBF) with a lower HCO_3^- concentration of 10 mmol/L[18,19], whereas *Takadama et al.* suggested, a newly improved SBF" (n-SBF) with HCO_3^- concentration of 4.2 mmol/L [20]. In a way, such propositions [18-20] confirmed the supremacy of Kokubo's con-SBF and represented a regressive step in the development of SBFs.

The drawbacks of most of the SBFs developed up to 2000s were as follows [21]: 1) they contained non-physiological buffering systems, such as tris-hydroxymethyl-aminomethane-HCl (TRIS-HCl) or 2-(4-(2-hydroxyethyl)-1-piperazinyl)ethane sulphonic acid-NaOH (HEPES-NaOH), which are not present in the normal human blood plasma, 2) they were utilized with total absence of HCO_3^- content regulation, although it was known that carbonates act as pH buffers in the human blood plasma and 3) they did not contain proteins, although it was known that proteins play a vital role in controlling the carbonated apatite formation.

The traditional TRIS-HCl and HEPES-NaOH buffering systems appeared to be ineffective in maintaining the longer-term pH [7,18,19,22-25] and chemical [18,21,23,24,26] stability of SBFs containing higher HCO_3^- concentrations, such as r-SBF [18]. In addition, the absence of HCO_3^- content regulation in SBFs enabled an uncontrolled CO_2 release from the SBFs into the ambient air causing the pH to increase with time (pH instability). Such pH instability increased the degree of supersaturation with respect to the homogeneous precipitation of carbonated apatite in SBF and affected the ion composition of the SBF (chemical instability).

The inability to maintain the physiological pH of r-SBF (and similar SBFs) for longer time intervals has sparked interest in replacing the traditional TRIS-HCl and HEPES-NaOH buffering systems. Since 2000, a number of studies investigated new systems for the SBF pH regulation using physiological CO_2/HCO_3^- buffering systems [22,27-32],

such as systems with continuous CO_2 bubbling into the SBF [22,28-30], closed systems with increased CO_2 partial pressure above the SBF [27,32], and systems with discontinuous CO_2 bubbling or "active pH regulation using CO_2" [31]. In contrast to SBFs buffered with traditional TRIS-HCl and HEPES-NaOH buffering systems, the new systems provide a higher level of pH and chemical stability of SBFs as well as the regulation of HCO_3^- content in SBFs. Moreover, the properties of derived apatitic phases were much closer to the bone-like apatite than the properties of the apatitic phases derived in Kokubo's con-SBF.

Regarding the effects of protein presence in SBFs, it is generally unknown how the proteins affect the pH stability of SBFs. There are no other data besides the few published articles that analyze/discuss the diffusion of CO_2 and other ion species in protein-containing solutions [33,34]. On the other hand, it is well known that proteins enhance the chemical stability of SBFs [29,32,33]. They inhibit the homogeneous nucleation of carbonated apatite within the bulk of SBFs [29,32,33]. However, different opinions exist regarding their influence on the formation of carbonated apatite on the surfaces of different model implants [29,32,33,35-41]. Such diversity of opinions could be the consequence of the utilization of different types and concentrations of proteins and/or different model implants.

In the present study, the major goals were to prepare the SBFs with natural buffers and to perform their evaluation. We prepared an initial, highly alkaline SBF with nominal inorganic ion composition close to that of the human blood plasma whose pH could be reduced to the physiological range by the simple addition of CO_2 (protein-free SBF) or a combination of CO_2 and model protein (protein-containing SBF). When needed, the pH of prepared SBFs was regulated between 7.2 and 7.6 by discontinuous addition of CO_2. During the evaluation stage, the pH and chemical instability of prepared SBFs were tested as well as the carbonated-apatite-forming ability on the surfaces of immersed model implants. More precisely, the specific goals were 1) to test the effects of a dissolved model protein, Ca^{2+} ions, and immersed plasma-sprayed HACs on the pH instability of prepared SBFs, 2) to test the effects of dissolved Ca^{2+} ions and model protein on the chemical instability of prepared SBFs, and 3) to test the effects of dissolved model protein on the carbonated-apatite-forming ability on the surfaces of immersed HACs. The pH stability testing was performed
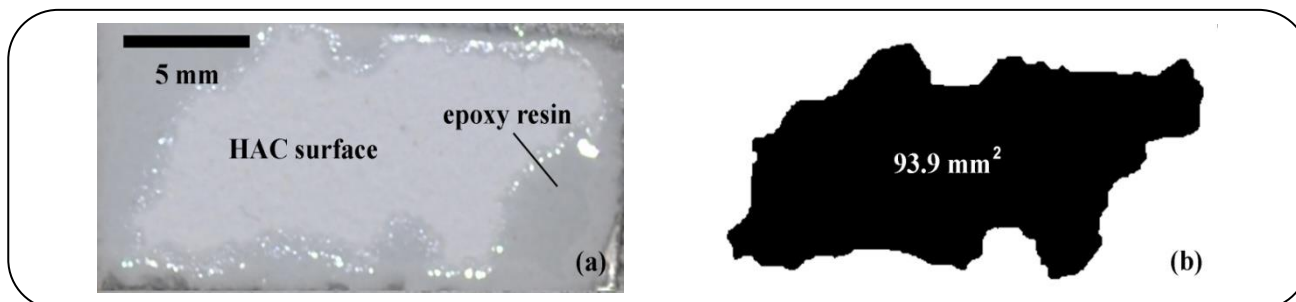
Fig. 1: (a) Typical macrograph of HACs for the immersion testing in the SBFs and (b) an example of the apparent surface area of HACs determined with ImageJ software.

in conditions of unregulated pH, whereas chemical instability and carbonated-apatite-ability testing was conducted under the conditions of both unregulated and regulated pH.

In contrast to most of the related studies, we have used the mixture of physiological concentrations of human gamma globulin (HGG) (33 g/L) and human serum albumin (HSA) (44 g/L) as the model protein, whereas the plasma-sprayed hydroxyapatite coatings (HACs) served as the model implants. The system for SBF pH regulation with discontinuous CO_2 addition was chosen because it mimics the mammalian respiratory function in contrast to other mentioned systems [22,27-30,32]. *Schinhammer et al.* have named this pH regulation method "active pH regulation using CO_2" [31]. Another reason for choosing this system is that it has not been evaluated in protein-containing SBFs and in the presence of plasma-sprayed hydroxyapatite coatings (HACs). The prepared SBFs and system for "active pH regulation utilizing CO_2" will be discussed for their strengths and shortcomings. The primary findings of the present study will be compared to the findings of other related studies.

EXPERIMENTAL SECTION
Preparation of HACs

The HACs were produced by using the high-power (52 kW) laminar plasma jet (Plasma Jet Co, Serbia) and the HA feedstock powder with a mean particle size of 90 ± 15 μm (Captal 90, Plasma Biotal, UK). The powder was plasma-sprayed onto the substrate made of the implantation-grade biomedical stainless steel AISI 316 LVM. The substrate material was in the form of plates with dimensions of 25 mm × 50 mm × 3 mm. The plasma spraying was performed at the stand-off distance of 100 mm from the substrate without preheating it. The details related to the plasma deposition process of HACs are given in previous

studies [42-44]. For immersion testing purposes, the HACs were cut to the sizes of 20 mm x 10 mm x 3 mm. The metallic part of the HACs was then protected with the epoxy resin to avoid direct contact between the metal substrate and the SBF during the immersion testing (Fig. 1a). During immersion testing, the apparent surface areas of HACs in direct contact with the SBF (in mm^2) differed from sample to sample. Using the HACs macrographs and ImageJ software, this variance was determined to be between 80 and 100 mm^2 [45]. (Fig. 1b)
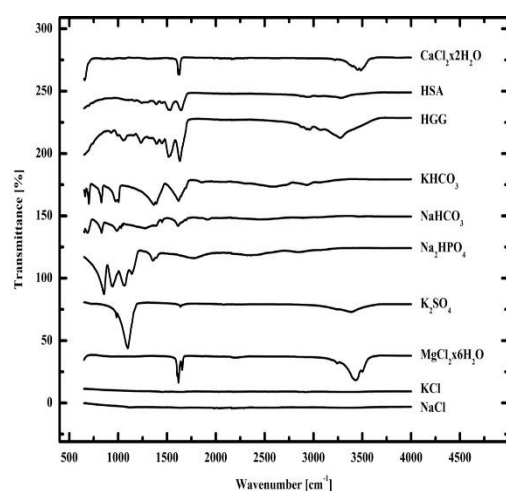
Reagents for SBFs

The SBFs were prepared by dissolving the analytical grade reagents in ultra-pure water (UPW) (Milli-Q System, Millipore, Billerica, MA, USA, 18.2 MΩ × cm). Table. 1 shows the order of addition of reagents in 100 mL of UPW, the types of reagents, and the amounts of dissolved reagents in 100 mL of UPW. Table. 1 also shows the nominal concentrations of the inorganic ions in the initial SBF solution, i.e. the nominal ion concentrations before the dissolution of CO_2, HGG, HSA, and $CaCl_2\times2H_2O$ into the UPW.

The reagents were in the form of powders, except for NaOH (3.75 mol/l UPW solution) and CO_2 (gas, purity 99.98 %) (Sigma Aldrich). Fig. 2 shows the infrared spectra of the powder reagents. The infrared spectra were obtained by using the attenuated total reflectance Fourier transform infrared (ATR-FTIR) spectrometry (Perkin Elmer Spectrum 100 with the Universal ATR accessory). The HGG (purity 99.0 %, moisture 1.1 %) and HSA (purity >98 %, moisture <2 %) were purchased from Golden West Biologicals, Inc., Temecula, CA, USA. The HGG and HSA lyophilized powders were supplied in sealed containers and were stored at a temperature of 2-8 °C.

Research Article

Table. 1: The order of reagents addition in UPW, types of reagents, the amounts of reagents dissolved in 100 mL of UPW, and nominal ion concentrations of the initial SBF solution.

Reagent No	Order of addition	Reagent	Amount	Ion	Nominal ion concentrations [mmol/L]
1		NaCl	0.64112 g	Na^+	141.0
2	1-4 (simultaneously)	KCl	0.00820 g	K^+	4.1
3		$MgCl_2 \times 6H_2O$	0.01626 g	Mg^{2+}	0.8
4		K_2SO_4	0.00871 g	Ca^{2+}	--
5	5	Na_2HPO_4	0.01420 g	SO_4^{2-}	0.5
6	6-7 (simultaneously)	$NaHCO_3$	0.12937 g	Cl^-	112.4
7		$KHCO_3$	0.02002 g	HCO_3^- (*)	17.4
8	8	3.75 mol/l-NaOH	0.371 mL	HPO_4^{2-}	1.0
9	9	CO_2	pH regulated	(*) – the presence of CO_3^{2-} (due to reaction of HCO_3^- with NaOH) is neglected at this point	
10	10	HGG	3.3000 g		
11	11	HSA	4.4000 g		
12	12	$CaCl_2 \times 2H_2O$	0.03381 g		

Fig. 2: ATR-FTIR spectra of solid-state reagents used for the preparation of SBFs.

Preparation of the initial SBF

The initial SBF was prepared in the following manner. 100 mL UPW was poured into a 200 mL glass beaker, which was then placed in a big flat glass beaker filled with technical water. The temperature of the technical water was previously set at 36.5-37.0 °C using a hot-plate magnetic stirrer and a flat glass beaker. When the 100 mL of UPW achieved the desired temperature, the reagents 1-4 (Table 1) were added simultaneously, followed by the dissolution of reagents 5, 6-7, and 8 in the order listed.

Pauses were taken in between phases to allow pH stabilization and complete reagent dissolution. The magnetic stirring speed was set to 250 rpm during the addition of chemicals to the UPW. Temperature and pH variations over time were regularly monitored. In addition, ATR-FTIR spectroscopy was used to track changes in the infrared spectra of the UPW solution after each group of reagents was dissolved.

The experimental setup

Fig. 3 shows the experimental setup used for the pH stability testing of SBFs and evaluation of carbonated-apatite-forming ability on the surfaces of immersed HACs.

The technical water was placed in the flat glass beaker, which was then placed on the hotplate magnetic stirrer. The thick plastic cover on top of the flat glass beaker was designed to allow for 1) uninterrupted contact between the SBFs and ambient air, 2) uninterrupted contact between the plastic vessels and the technical water from the flat glass beaker, and 3) sufficient access for the pH electrodes, thermometers, and reagents addition. The top thick plastic cover had four openings. Each opening was sealed from one side with the 40 mL plastic vessel by using epoxy resin. The established epoxy joints between the plastic vessels and the top thick plastic cover were cured in the furnace for 24 h at 45 °C. After curing, the flat glass beaker was covered with the top thick plastic cover, as shown in Fig. 3.
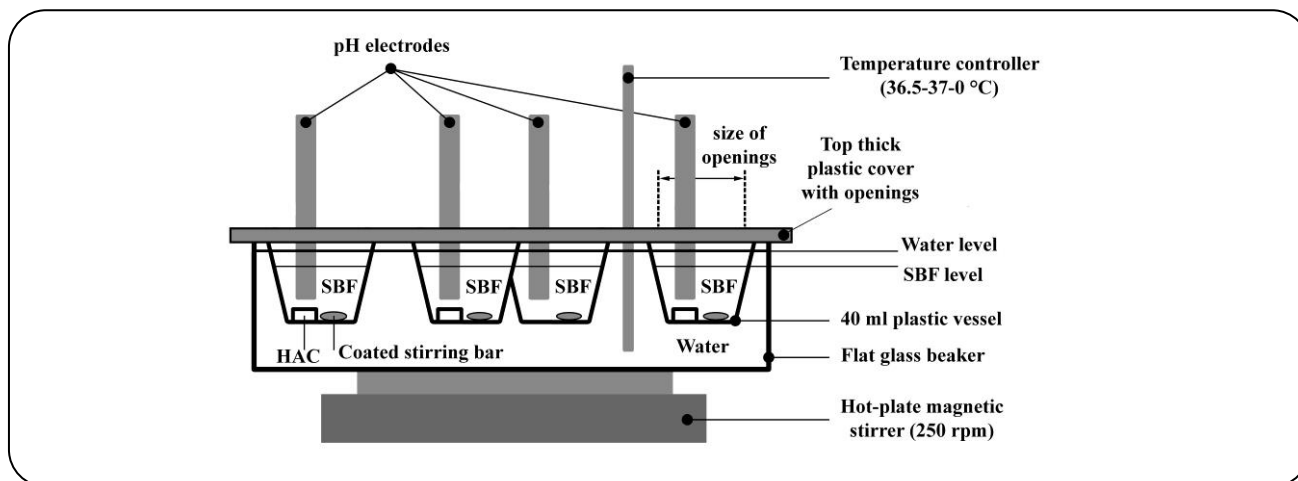
Fig. 3: The experimental setup.

Prior to experiments, all glass and plastic vessels and other laboratory accessories that came in contact with SBFs were thoroughly washed (acetone, hydrochloric acid, and UPW) and dried in a furnace at 120 °C in the air for at least 24h. Throughout all of the experiments, the temperature controller was adjusted to keep the technical water in the flat glass beaker between 36.5 and 37.0 °C, while magnetic stirring was performed at 250 rpm with coated stirring bars.

The pH instability testing of SBFs

Experiments without a system for active pH regulation using CO_2 were carried out to assess the pH instability of SBFs under various experimental conditions (in the presence and absence of human proteins, with and without the addition of $CaCl_2 \times 2H_2O$, in the absence and presence of immersed HACs). Each SBF's pH instability testing lasted 4 hours and was conducted twice to ensure consistency.

Four portions of the initial SBF (25 mL each) (Table. 1) were passed through the fiberglass filters (Millipore) and transferred into the 40 mL plastic vessels (Fig. 3). In two of four plastic vessels (Fig. 3), the pH of the initial SBFs was reduced from 10.5±0.3 to 7.2 by the simple addition of gaseous CO_2. The pH of the initial SBF was first decreased from 10.50.3 to 8.3 using CO_2 in the remaining two plastic vessels (Fig. 3), where the effects of the human protein presence were tested. Subsequently, HGG (3.3 g/dl), HSA (4.4 g/dl), and small amounts of gaseous CO_2 were immediately added, and a pH of 7.2 was achieved. It should be mentioned that the pH of 7.2 was used as the starting pH for all pH stability testing experiments carried out in the present study. The addition of CO_2 was regulated by observing the changes in pH. It was performed in consecutive steps, i.e. the pH of the initial SBFs (10.5±0.3) was reduced to 8.3 (or 7.2) in steps of 0.2 pH units. After each pH reduction step, the addition of CO_2 was temporarily terminated to allow the short stabilization of pH to a certain intermediate value. The addition of human proteins into the SBFs was aided by mechanical stirring to accelerate their dissolution.

To evaluate the effects of Ca^{2+} ions on the pH and chemical instability of SBFs, the experiments were performed in the absence of the Ca^{2+} ions in one protein-containing SBF and one protein-free SBF, (without the addition of $CaCl_2 \times 2H_2O$). In the remaining protein-containing SBF and protein-free SBF, the experiments were performed in the presence of the Ca^{2+} ions (with the addition of 2.3 mmol/L of $CaCl_2 \times 2H_2O$). $CaCl_2 \times 2H_2O$ was always added in the final step when the pH of SBFs was established at 7.2 to avoid the apatite homogeneous precipitation process at higher pH. Small portions of dissolved $CaCl_2 \times 2H_2O$ in UPW were added in the area around the rotating coated stirring bars located in the SBFs at the bottom of the plastic vessels. It was done to enable fast distribution of Ca^{2+} ions throughout the entire volume of SBFs to avoid the occurrence of local apatite precipitation.

Evaluation of carbonated-apatite-forming ability on the surfaces of immersed HACs

Evaluation of the carbonated-apatite-forming ability on the surfaces of immersed HACs was performed under different experimental conditions (without and with a system for active pH regulation using CO_2 and in the presence and

absence of human proteins). Four portions of the initial SBF (20 to 30 mL each) (Table. 1) were passed through the fiberglass filters (Millipore) and transferred into the 40 mL plastic vessels (Fig. 3) for further treatment. The exact volumes of the initial SBF were determined with respect to the apparent surface areas of the HACs that were in direct contact with the SBF during the immersion testing (Fig. 1b). In all cases, the ratio of the apparent surface area to the volume of the initial SBF was 4 mm^2/mL. In the previous study of *Kokubo* and *Takadama* [8], the ratio of 10 mm^2/mL has been used for the carbonated-apatite-forming ability testing. For consistency, each carbonated-apatite-forming ability test was repeated twice.

The pH of the four initial SBFs (10.5±0.3) was reduced to 7.2 by following the same procedure as for the pH stability testing of SBFs explained in the previous section. In this way, two protein-free SBFs and two protein-containing SBFs were produced. CO_2, CO_2/protein combination, and $CaCl_2 \times 2H_2O$ were added in the initial SBFs using the same concentrations and by following the same procedures. In contrast to pH stability testing experiments where $CaCl_2 \times 2H_2O$ reagent was added in only two SBFs to observe its effects on pH changes with time in the presence and absence of human proteins, $CaCl_2 \times 2H_2O$ reagent was added in each of four SBFs to achieve their full nominal ion composition in this stage of the investigation.

When pH of 7.2 of four SBFs was established after the addition of CO_2 or CO_2/human proteins combination and when the $CaCl_2 \times 2H_2O$ was added in four SBFs, the testing of carbonated-apatite-forming ability on the surfaces of HACs started after the immersion of four HACs into the four prepared SBFs. The pH was set to change with time without the system for active pH regulation using CO_2 (unregulated pH) in one protein-containing and one protein-free SBF. The pH was maintained between 7.2 and 7.6 using CO_2 (the experiments with the system for active pH regulation using CO_2) (regulated pH) in the remaining protein-containing and protein-free SBF. Each time when pH value was increased from 7.2 to 7.6, the CO_2 was added immediately to reduce the pH from 7.6 back to 7.2. After 20 h of immersion testing, the HACs were withdrawn from the SBFs and were dried in ambient air at room temperature.

Characterization of the SBFs and HACs

The pH measurements were performed by using the four Docu-pH Meters (Sartorius) simultaneously. The pH electrodes were calibrated against the standard solutions at 4, 7, and 9 pH units prior to each series of measurements. The measurement accuracy of the pH meters was 0.01.

The changes in the UPW solutions throughout the preparation of SBFs were observed using ATR-FTIR spectrometry. More precisely, the ATR-FTIR was used to observe variations in SBFs that were associated with hydrated carbon species. The Perkin Elmer Spectrum 100 with the Universal ATR accessory was used to perform the ATR-FTIR measurements. The UPW's background spectrum was recorded before each series of measurements. A droplet of UPW was placed on the cleaned diamond top plate to get the background spectrum. The same approach was used to acquire the ATR-FTIR spectra of SBFs. An average of 16 scans with a resolution of 4 cm^{-1} was used to create each spectrum. At room temperature in ambient air, all ATR-FTIR spectra were obtained in the range of 650-4000 cm^{-1}. The ATR-FTIR spectrometer was also utilized to confirm the type of powder reagents used to prepare the SBFs, as previously described.

Using a sharp metallic tool, 2 mg of the sample material for the analysis was removed from the surface of each HAC after immersion testing in the SBFs and drying in ambient air at room temperature. The removed material was then mechanically homogenized with 200 mg of KBr powder that had previously been dried in the furnace at 110 °C in the air for 24 hours. Using a 15 t hydraulic press, the homogenized mechanical mixtures of sample and KBr powders were compressed into pellets. The pellets were transparent, measuring 1 cm in diameter and 1 mm in thickness. The pellets were stored in a desiccator prior to analysis. The transmission FT-IR (T-FTIR) measurements were carried out in ambient air using the FTIR BOMEM Hartman Braun MB series at room temperature. The 400-4000 cm^{-1} range was used to collect all T-FTIR spectra. Each spectrum was created by averaging ten scans with a resolution of 4 cm^{-1}.

RESULTS AND DISCUSSION
Preparation of SBFs

To determine how each reagent affected the ATR-FTIR spectra of UPW after dissolution, or to obtain the reference ATR-FTIR spectrum for each dissolved reagent, ATR-FTIR spectra from 100 times concentrated UPW solutions of reagents were analyzed (Fig. 4). Water bending bands (1632 cm^{-1}) and water absorption bands
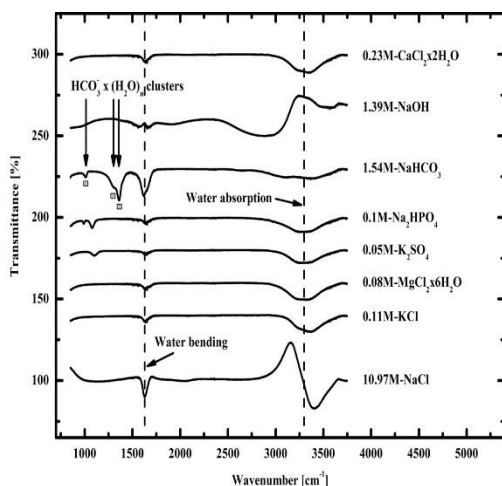
Fig. 4: The ATR-FTIR spectra of highly concentrated UPW solutions of reagents (100 × SBF). M represents mol/l.

Fig. 5: The changes in the ATR-FTIR spectra and pH during the preparation of SBFs.

were visible in all ATR-FTIR spectra (2800-3700 cm^{-1}). Only the NaHCO$_3$ (and KHCO$_3$) spectra revealed prominent bands between 1100 and 1500 cm^{-1}, out of all the spectra. The presence of HCO$_3^-$(H$_2$O)$_n$ clusters was attributed to the presence of a strong peak at 1362 cm^{-1}, a shoulder at 1305 cm^{-1}, and a small peak at 1010 cm^{-1} in the spectra of NaHCO$_3$ solution. These bands have been reported in the study of infrared spectroscopy of the hydrated bicarbonate anion clusters [46].

The first set of reagents dissolved in the UPW (1-4, Table 1) produced an electrolyte solution with a pH between 6.6 and 7.2. (Fig. 5). The dissolution did not promote the appearance of ATR-FTIR bands between 1100 and 1500 cm^{-1}, which was consistent with the ATR-FTIR spectra of the highly concentrated reagent solutions (Fig. 4). The addition of Na$_2$HPO$_4$ (5, Table 1) raised the pH of the electrolyte solution to between 8.3 and 8.5. (Fig. 5). Other than a slight decrease in the integrated intensity of the water bending band at 1632 cm^{-1}, other changes in the ATR-FTIR spectra were imperceptible. The addition of NaHCO$_3$ and KHCO$_3$ (6-7, Table 1) reduced the alkalinity of the electrolyte solution to between 8.1 and 8.3. The ATR-FTIR spectra revealed the presence of a band at 1362 cm^{-1} (Fig. 5). Previously, this band was associated with the presence of HCO$_3^-$(H$_2$O)$_n$ clusters (Fig. 4 and [46]). There was also an increase in the integrated intensity of the water bending band at 1632 cm^{-1}. The addition of NaOH increased the pH of the electrolyte solution to 10.5±0.3, altering the equilibrium between the hydrated carbon species (CO$_{2(aq)}$,
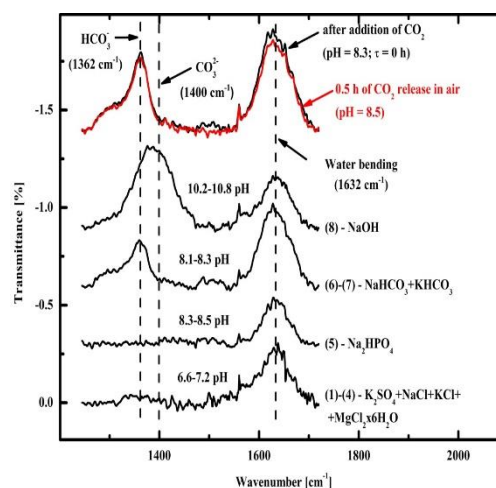
HCO$_3^-$$_{(aq)}$, and CO$_3^{2-}$$_{(aq)}$). The amount of NaOH added to the electrolyte solution (13.9 mmol/L) was less than the amount of HCO$_3^-$ already present (17.4 mmol/L) (Table. 1). The larger portion of HCO$_3^-$ (>50%) reacted with NaOH to form CO$_3^{2-}$. The appearance of the band at 1400 cm^{-1} in the ATR-FTIR spectra was caused by the formation of CO$_3^{2-}$ (Fig. 5). Furthermore, the addition of NaOH resulted in a significant decrease in the integrated intensity of the water bending band at 1632 cm^{-1}.

The initial SBF had a significant amount of CO$_3^{2-}$ ions and had a pH that was significantly above the physiological pH of 7.4 [5-8] after adding NaOH. Using CO$_2$, the high pH of 10.5±0.3 was easily lowered to 7.2. However, simply adding the human (HGG+HSA) protein mixture did not reduce the pH to 7.2. Further investigations demonstrated that adding human proteins with concentrations near to normal levels (3.3 g/dl of HGG and 4.4 g/dl of HSA [5,6,47]) could enhance the decrease of pH from 8.3-8.4 to 7.3-7.4. This advantage was further exploited. The pH of 10.5±0.3 was first reduced to 8.3 by using CO$_2$.

When CO$_2$ was added to lower the pH from 10.5.0.3 to 8.3, the CO$_3^{2-}$ band at 1400 cm^{-1} vanished, but the HCO$_3^-$ band at 1362 cm^{-1} was completely restored (Fig. 5). At 1362 cm^{-1}, the integrated intensity of the water bending band rose by just 10-15%. The integrated intensity of the HCO$_3^-$ band was 50-60% higher than it was previous to the addition of NaOH, which was consistent with the distribution of carbon species (CO$_{2(aq)}$, HCO$_3^-$$_{(aq)}$, and CO$_3^{2-}$$_{(aq)}$) under physiological conditions [48]. Due to CO$_2$
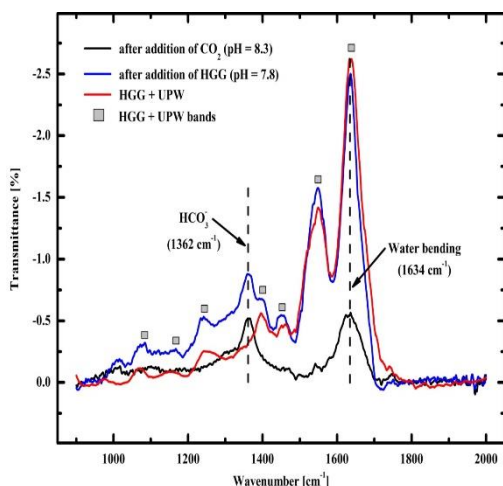
Fig. 6: The effects of HGG addition on the appearance of ATR-FTIR spectra and pH changes during the preparation of SBFs.

release from the SBF into the ambient air, the pH was unstable after 0.5 hours and shifted from 8.3 to 8.5. This change was observable in the ATR-FTIR spectra. The integrated intensities of the water bending band at 1632 cm⁻¹ and the HCO_3^- band at 1362 cm⁻¹ slightly decreased after 0.5 h (Fig. 5). Because of the observed pH instability, the HGG+HSA protein mixture was added to the SBFs soon after the CO_2 was added, i.e. after the pH was reduced from 10.5±0.3 to 8.3. Usually, the HGG was added first.

The addition of HGG increased the acidity of the electrolyte solution from pH of 8.3 to 7.7-7.8 (Fig. 6). Based on the appearances of the resultant ATR-FTIR spectra, the spectral lines of the HGG solution into UPW (HGG+UPW) were superimposed onto those observed after CO_2 addition, i.e. after pH changed from 10.5±0.3 to 8.3. This result indicated that the addition of HGG had no significant effect on HCO3- concentration. The acidity of solutions was further increased by the dissolution of HSA, which decreased the pH from 7.7-7.8 to 7.3-7.4. Although not presented, HCO_3^- concentration was also insignicantly affected. CO_2 was added for a short time interval after HSA dissolution to achieve the starting pH of 7.2.

Instability of SBFs
SBFs without the presence of Ca^{2+} ions and HACs (the pH instability)

During the 4 h of pH instability testing, Ca^{2+}-free protein-free SBFs remained transparent. The homogeneous precipitation was visually imperceptible in

protein-free SBFs. Protein-containing SBFs, on the other hand, were opaque. There was no observable evidence of a homogeneous precipitation process.

In both protein-free and protein-containing SBFs, the pH increased significantly with time (Fig. 7a). The pH of protein-free and protein-containing SBFs increased with time at rates of 1.2-1.7 pH units/h and 0.4-0.8 pH units/h, respectively, within the 7.2-8.0 pH range. In other words, protein-containing SBFs' pH increased at a 60 % slower rate over time.

Table 2 compares the pH instability results of the current study with those of other relevant research. SBFs buffered with HEPES-NaOH and TRIS-HCl exhibit the highest pH stability [18,23,49]. In the case of both buffering systems, the pH increase with time is of the same order of magnitude (10^{-4} pH units/h) [18,23,49]. The pH instability increases when CO_2 is added to the SBF that already contains TRIS-HCl buffering system [23,24]. The pH increase with time is higher by at least one order of magnitude [23,24]. When the TRIS-HCl buffering system is eliminated from the previous system but CO_2 addition is kept as an option, pH instability increases even more [24,25]. The pH increase with time rises by another order of magnitude [24,25]. By removing the CO_2 addition in the last system, the pH instability reduces [25,30]. The pH increase with time becomes 6-7 times lower. These comparisons show that CO_2 addition significantly reduces the pH stability of SBFs under the ambient air, regardless of the presence of the TRIS-HCl or HEPES-NaOH buffering system.

According to Table. 2, the pH instability of the SBFs prepared in the present study appears to be the highest. It should be noted, however, that the SBFs in Ref. [25,30] have 5 times greater ionic strengths. The solubility of CO_2 in the SBF and the pH-time profile of the SBF are affected by higher ionic strength [25,30]. Therefore, the experimentally determined pH increases with time more likely indicate natural rather than the highest pH instability of the SBFs prepared in the present study.

The differences in pH increase with time observed in protein-containing and protein-free SBFs (Fig. 7a) were attributable mostly to changes in CO_2 diffusivity in the presence and absence of dissolved HGG+HSA in the SBF. The diffusion coefficient of CO_2 in albumin-containing water solutions is greatly influenced by CO_2 partial pressure [34]. The diffusion coefficient of dissolved CO_2 in albumin-containing water solutions is 30-35 % lower

Table 2: The pH instability of r-SBF-like [18] solutions under the ambient air environment: present work vs. other related studies.

Ref/Year	Temperature [°C]	Buffering system / Addition of CO_2	Protein presence	Initial pH/ Intermediate pH (**)	Time interval (***)	pH increase with time [pH units/h]
[18] / 2002	36.5	HEPES-NaOH / No	No	7.40/7.55	8 w	1.11×10^{-4}
[25] / 2002(*)	37.0	No / Yes	No	6.20/6.70	4.50 h	1.11×10^{-1}
[23] / 2006	37.0	TRIS-HCl / No	No	7.30/7.62	14 d	9.52×10^{-4}
[24]/ 2008	40.0	TRIS-HCl / Yes	No	6.49/6.64	9.00 h	1.66×10^{-2}
[30] / 2011(*)	37.0	No / No	No	6.40/8.00	24.00 h	6.67×10^{-1}
[49] / 2017	36.5	HEPES-NaOH / No	No	7.40/8.00	8 w	4.46×10^{-4}
Present work / 2021	36.5-37.0	No / Yes	No	7.20/8.00	0.65 h	1.23×10^{0}(****)
Present work / 2021	36.5-37.0	No /Yes	Yes	7.20/8.00	2.00 h	4.00×10^{-1}(****)

(*) – SBF contained 5× ion concentration compared to classical Kokubo SBF formulations; (**) – Intermediate pH of SBF refers to pH which was reached after certain time interval and which was taken as a value to estimate pH increase with time; (***) – h-hours, d-days, w-weeks; (****) – Values correspond to Ca^{2+}-containing protein-free and protein-containing SBFs with full nominal ion compositions (Fig.7a).
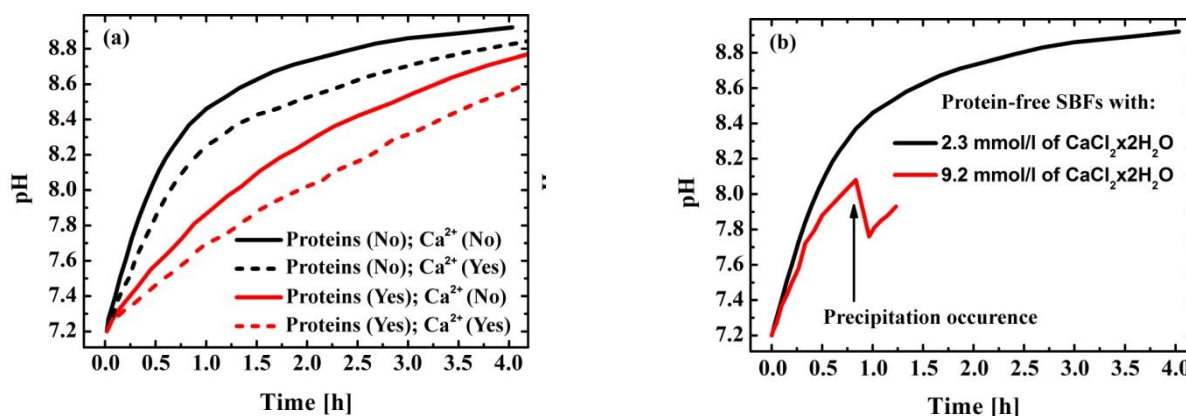
Fig. 7: The evolution of pH with time in the experiments without a system for active pH regulation using CO_2 and without the presence of immersed HACs (a) where the presence of human proteins and Ca^{2+} ions in SBFs were combined and (b) where four times higher concentration of Ca^{2+} ions in protein-free SBFs was added. In Fig. 7a Proteins (No) and Proteins (Yes) designate the protein-free and protein-containing SBFs, respectively, whereas Ca^{2+} (No) and Ca^{2+} (Yes) designate the absence and presence of dissolved $CaCl_2 \times 2H_2O$ in SBFs, respectively.

then in pure water at higher CO_2 partial pressures (>18.6 kPa) [34]. Furthermore, protein-containing SBFs have higher density/viscosity than protein-free SBFs [33], limiting ion and another species diffusion in the SBF [33].

HGG+HSA buffer capacity was also attributed (to some extent) to the 60 % lower pH increase with time in protein-containing SBF compared to protein-free SBF (Fig. 7a). Within the physiological pH range, bovine serum albumin (BSA) in SBFs has been found to have a limited buffer capacity [50]. Furthermore, at pH>8.5, which is outside of the physiological pH range, the BSA buffer capacity steadily increases [50]. Nonetheless, due to the acidic effect of HGG and HSA dissolution observed during SBF preparation, a little contribution of HGG+HSA buffer capacity cannot be ruled out in the current study.

SBFs with the presence of Ca^{2+} ions and without the presence of HACs (the chemical instability)

After 0.6-1 h, Ca^{2+}-containing protein-free SBFs became slightly cloudy. The homogenous precipitation process within the bulk of the SBFs was visually

Research Article

Table 3: The chemical instability of r-SBF-like [18] solutions: present work vs. other related studies.

Ref/Year	Temperature [°C]	Buffering system / Addition of CO_2	Protein presence	Comments on SBF stability towards a homogenous nucleation of apatitic calcium phosphate
[18] / 2002	36.5	HEPES-NaOH / No	No	SBF remained stable up to 2 w
[23] / 2006	37.0	TRIS-HCl / No	No	SBF remained clear even after 2 w
[24] / 2008	40.0	TRIS-HCl/Yes	No	SBF with the initial pH of 6.81 became cloudy after 4.5 h
[30] / 2011(*)	37.0	No / No	No	SBF became cloudy after 1 h
[33] / 2012	37.0	HEPES-NaOH / No	Yes	Proteins inhibit homogeneous nucleation of apatitic calcium phosphate
[49] / 2017	36.5	HEPES-NaOH / No	No	SBF remained stable up to 1 w
[32] / 2017	37.0	TRIS-HCl / No	Yes	Proteins inhibit homogeneous nucleation of apatitic calcium phosphate
Present work / 2021	36.5-37.0	No / Yes	No	SBF with an initial pH of 7.2 became cloudy after 0.6-1.0 h
Present work / 2021	36.5-37.0	No / Yes	Yes	Could not be estimated due to the opacity of protein-containing SBF

(*) – SBF contained 5× ion concentration compared to classical Kokubo SBF formulations

confirmed. Because of their opacity, homogenous precipitation in protein-containing SBFs was inconclusive.

The addition of Ca^{2+} ions lowered the rate of pH increase with time by 15% in protein-free SBFs and 25% in protein-containing SBFs within the 7.2-8.0 pH range (Fig. 7a). The slower pH increase with time in protein-free SBFs was attributed to the homogeneous carbonated apatite precipitation process [18,23,51,52], whereas a slightly slower pH increase with time in protein-containing SBFs was attributed to both homogeneous carbonated apatite precipitation [18,23,51,52] and low buffer capacity of HGG+HSA [50]. The apatite precipitation reaction causes a release of hydronium ions (H_3O^+) [25] or consumption of hydroxide ions (OH^-) [24] in the SBFs. This reaction counteracts the increase of pH with time caused by the CO_2 release from the SBFs into the ambient air. As a result, a slower overall pH increase with time was observed in Ca^{2+}-containing SBFs than in Ca^{2+}-free SBFs (Fig.7a).

The homogeneous precipitation process of carbonated apatite is frequently related to the sudden pH drop [24], which remained undetected in SBFs containing 2.3 mmol/L of $CaCl_2 \times 2H_2O$ (Fig.7a). However, the addition of 9.2 mmol/L $CaCl_2 \times 2H_2O$ caused a rapid reduction in pH (Fig.7b) and considerable blurring of protein-free SBFs. This result clearly indicated the homogeneous precipitation of carbonated apatite. Therefore, although the abrupt pH drop with time was imperceptible in SBFs containing 2.3 mmol/L of $CaCl_2 \times 2H_2O$, a 15 % slower pH increase with time compared to the Ca^{2+}-free SBFs

(Fig.7a) was attributed to the early stages of homogeneous precipitation of carbonated apatite, i.e. the early formation of the ionic clusters [51,53].

Table. 3 compares the chemical instability results derived in the present work with the results reported in other related studies. Similar to the pH instability (Table 2), the chemical instability of SBFs buffered with TRIS-HCl or HEPES-NaOH buffering systems is lowest, whereas the chemical instability of SBFs buffered with physiological CO_2/HCO_3^- the buffering system is highest. Because the degree of supersaturation toward homogenous precipitation of carbonated apatite in SBFs increases abruptly with pH [23], it becomes clear that pH instability has a direct impact on the chemical instability of SBFs. Therefore, regarding the SBFs prepared in the present work, the addition of 2.3 mmol/L of $CaCl_2 \times 2H_2O$ should be undertaken only when the pH of SBFs prepared with natural buffers is maintained within the physiological range (7.4).

SBFs with the presence of Ca^{2+} ions and HACs

In the experiments without a system for active pH regulation using CO_2 (unregulated pH), the pH of the protein-containing SBFs grew at a 50-70 percent slower rate than that of the protein-free SBFs within the 7.2-8.0 pH range when the HACs were immersed in the SBFs (Fig. 8a). This result was similar to the result previously observed in the SBFs without the presence of HACs (Fig. 7a). In the experiments with the system for active pH regulation
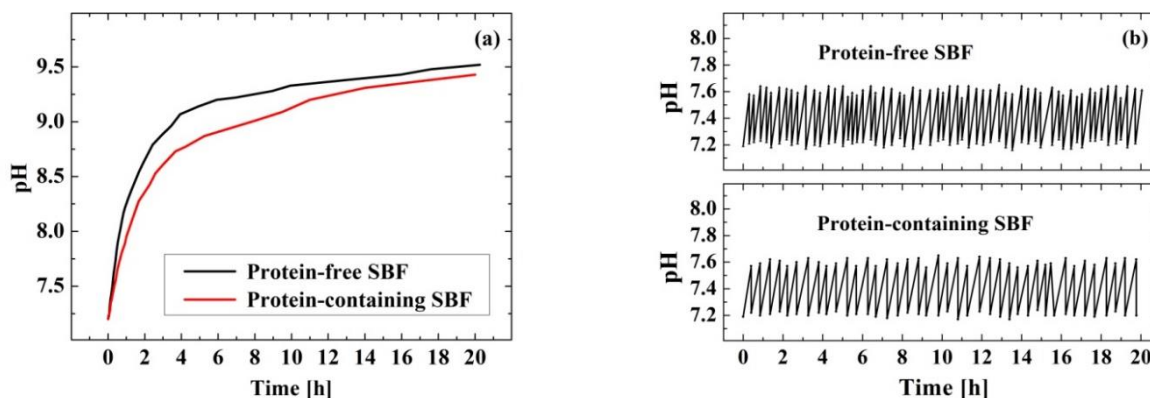
Fig. 8: The evolution of pH with time in the experiments without (a) and with (b) system for active pH regulation using CO₂ in the presence of immersed HACs.

using CO_2 (regulated pH), CO_2 was added less frequently to the protein-containing SBFs (every 30 ± 6 min) than to the protein-free SBFs (every 20 ± 6 min) to adjust the pH between 7.2 and 7.6 (Fig. 8b).

The protein-free SBFs became slightly cloudy after 1 h of HACs immersion testing in the experiments with unregulated pH (Fig. 8a). They retained this state for the remainder of the 19 h immersion testing period. The protein-free SBFs, on the other hand, were transparent during the whole period of HACs immersion testing in the experiments with regulated pH (20 h) (Fig. 8b).

Carbonated-apatite-forming ability on the surfaces of immersed HACs

Fig. 9 shows T-FTIR spectra of samples taken from the surfaces of HACs in the initial condition (prior to immersion testing in SBFs). Fig. 9 also shows T-FTIR spectra of samples taken from surfaces of HACs after immersion testing in the protein-free and protein-containing SBFs with (regulated pH) and without (unregulated pH) system for active pH regulation using CO_2. Low integrated intensities of CO_3^{2-}, OH^-, and amide bands between 1300 and 1800 cm^{-1} in Fig. 9 are illustrated in detail in Fig. 10.

HAC initial condition

T-FTIR spectra of samples collected from the surfaces of HACs in the initial condition showed the presence of the infrared bands at 571 and 603, 962, and 1050 and 1090 cm^{-1} (Fig.9). These bands were assigned to the bending mode (υ_4), symmetric stretching mode (υ_1), and asymmetric stretching mode (υ_3) of PO_4^{3-} groups in

hydroxyapatite, respectively. The bands located at 1630 and 3567 cm^{-1} were attributed to the OH^- bending and stretching modes of the absorbed water, respectively. The absorbed water appeared as a broad band between 3100 and 3700 cm^{-1}. The bands located at 2852 and 2920 cm^{-1} were assigned to $-CH_2-$ stretching mode. The locations of all mentioned infrared bands have also been reported in earlier studies [54-56]. Here it should be mentioned that infrared bands found in the case of HACs in the initial condition were also detected in all samples taken from the surfaces of all HACs that were immersed in protein-free and protein-containing SBFs. Therefore, these bands will not be addressed in the further analysis.

Experiments without the system for active pH regulation using CO_2 (unregulated pH)

T-FTIR spectra obtained from samples collected from the surfaces of HACs, which were immersed in protein-free SBFs, showed bands at 876 and at 1420, and 1495 cm^{-1} (Fig. 9 and Fig. 10). These bands were assigned to bending and asymmetric stretching modes of CO_3^{2-} [54-57], respectively. The last strongly suggested that carbonated apatite was formed on the surfaces of HACs during the immersion testing

T-FTIR spectra of samples taken from the surfaces of HACs, which were immersed in protein-containing SBFs, revealed the presence of an amide I band at 1652 cm^{-1} and an amide II band at 1548 cm^{-1} (Fig. 9 and Fig. 10). It was an indicator that human proteins were adsorbed on the surfaces of HACs during the immersion testing. The presence of these amide bands has been documented in previous investigations [35,36,58]. The amide I band
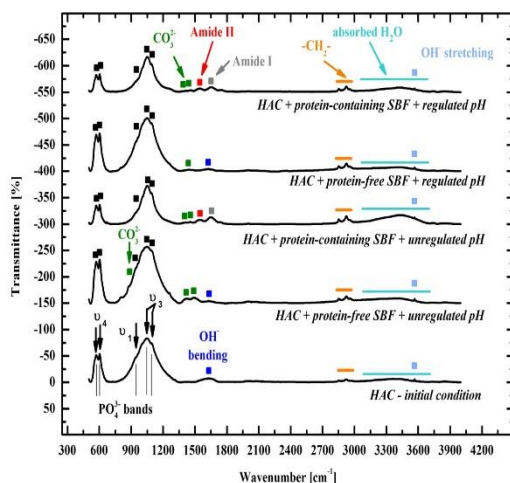
Fig. 9: The effects of protein presence and the type of pH regulation on the appearance of the T-FTIR spectra derived from the powders collected from the surfaces of the HACs after their immersion into the SBFs. "Unregulated pH" refers to experiments performed without the system for active pH regulation using CO2, whereas regulated pH refers to experiments performed with the system for active pH regulation using CO2.
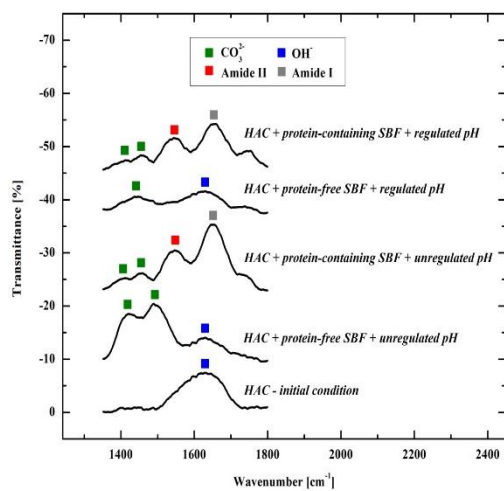
Fig. 10: Part of the T-FTIR spectra from Fig. 9 showing detailed changes in intensities of CO_3^{2-}, OH^-, and amide infrared bands.

at 1652 cm^{-1} most likely overlapped with the OH-bending band of the absorbed water (Fig. 10) [35]. T-FTIR spectra examination revealed CO_3^{2-} bands at 1410 and 1455 cm^{-1} (Figs. 9 and 10), indicating that, in addition to adsorbed human proteins, carbonated apatite was produced on the

surfaces of the HACs during the immersion testing. The human proteins hindered the development of carbonated apatite, as evidenced by the decreased integrated intensity of these CO_3^{2-} bands compared to the protein-free SBFs.

In general, the formation of carbonated apatite in SBFs with immersed HACs may occur at two main locations. The first location is on the surfaces of HACs or other substrates, where carbonated apatite forms by nucleation and growth mechanism [23-25,28,29,33,35,36,58], whereas the second location is within the bulk of the SBFs, where carbonated apatite forms through a homogeneous precipitation process [23,33,51]. Analogously, human proteins may affect the formation of carbonated apatite in two ways. The first is the protein adsorption on the surfaces of HACs, and the second is the protein interaction with inorganic ions and ion clusters within the bulk of the SBFs [33].

Albumin adsorption may be mediated through electrostatic interactions between the albumin's COOH$^-$ groups and the Ca^{2+} HAC surface ions [58]. Another possibility is that its NH$_3^+$ groups interact with PO$_4^{3-}$ HAC surface ions [58]. Protein adsorption can affect the formation of carbonated apatite by altering the interfacial energy between the HAC substrate and the SBF [33]. The interaction between proteins and free inorganic ions and ion clusters within the bulk of the SBFs (complexation), on the other hand, is also important for the formation of carbonated apatite [59,60]. The lowering of free Ca^{2+} concentration in the SBF caused by Ca^{2+} complexation with proteins may decrease the amount of Ca^{2+} needed for the formation of carbonated apatite [33]. Furthermore, proteins enhance the viscosity/density of the SBF, which impacts the diffusion of Ca^{2+}, phosphorus, and carbon species, potentially inhibiting the formation of the carbonated apatite on the substrate surfaces [33]. In the present study, T-FTIR spectra revealed that the presence of HGG+HSA in physiological amounts (3.3 g/dl of HGG and 4.4 g/dl of HSA) inhibited the formation of the carbonated apatite on the surfaces of the HACs in SBFs with unregulated pH.

Experiments with the system for active pH regulation using CO_2 (regulated pH)

T-FTIR spectra obtained from samples collected from the surfaces of HACs, which were immersed in protein-free SBFs, exhibited weak infrared CO_3^{2-} band at 1450 cm^{-1}

(Fig. 9 and Fig. 10). This band suggested that the carbonated apatite was formed on the surfaces of HACs during the immersion testing. The lower integrated intensity of this infrared CO_3^{2-} band compared to the higher integrated intensity of infrared CO_3^{2-} band derived in experiments with unregulated pH in protein-free SBFs demonstrated a significantly different outcome of the in-vitro testing of HACs when the system for active pH regulation was applied.

The presence of amide I and II bands in T-FTIR spectra obtained from samples taken from the surfaces of HACs immersed in protein-containing SBFs suggested that the proteins were adsorbed on the surfaces of HACs during the immersion testing. In addition, the CO_3^{2-} bands at 1410 and 1455 cm^{-1} revealed that carbonated apatite was produced on the surfaces of HACs (Fig. 9 and Fig. 10). The detection of CO_3^{2-} and amide infrared bands, similar to the experiments with protein-containing SBFs with unregulated pH, indicated that carbonated apatite formation and protein adsorption were simultaneous processes [29,37] The integrated intensity of the CO_3^{2-} bands, however, did not indicate that the protein presence hindered the formation of carbonated apatite, as seen in the SBFs with unregulated pH. In comparison to protein-free SBFs, the integrated intensity of CO_3^{2-} infrared bands was somewhat higher in protein-containing SBFs (Fig. 10). Therefore, in the present study, HGG+HSA protein presence either had no effect on the formation of carbonated apatite on the surfaces of immersed HACs or had a beneficial effect.

Effects of protein presence on the carbonated-apatite-forming ability

Table 4 compares the effects of protein presence on the carbonated-apatite-forming ability on the surfaces of plasma-sprayed HACs observed in the present work with the effects reported in other related studies. Regardless of different substrates, the comparison shows the inhibitory effects of protein BSA presence in Kokubo's c-SBF with 4.2 mmol/L of HCO_3^- buffered with TRIS-HCl buffering system [32,37].

The favorable effects of protein presence are reported when the TRIS-HCl buffering system of the Kokubo's c-SBF is replaced by a CO_2/HCO_3^- buffering system with continuous CO_2/N_2 bubbling [29] or when the Kokubo's c-SBF without TRIS-HCl is placed under a 5% CO_2

environment (Table 3) [32]. *Marques et al.* have compared mineralization effects in BSA-containing and BSA-free SBFs containing 24-27 mmol/L of HCO_3^- both buffered with CO_2/HCO_3^- buffering system [29]. They have concluded the same favorable effects. The mineralization effect is stronger in the BSA presence due to its incorporation in the deposited carbonated apatite layer [29]. Contrarily, *Zhao et al.* have increased BSA concentration from 0.1 g/L and reached the full inhibitory effect of BSA at 5 g/L in SBFs containing 22-23 mmol/L of HCO_3^- placed under the 5% CO_2 atmosphere [32]. They have concluded that the formation of carbonated apatite on the surfaces of model implants depends on the protein concentration [32].

Very few studies have used higher concentrations of BSA in SBFs containing 27 mmol/L of HCO_3^- [33,39] (Table 4). Unfortunately, their SBFs contained HEPES-NaOH [33] or TRIS-HCl [39]. In the first case, the effect of BSA has been termed inhibitory based on the assumption that a higher density of protein-containing SBFs retards the diffusion of dissolved calcium, phosphorus, and carbon species [33]. In the second case, the BSA has produced insignificant effects in-vitro, and the nucleation and growth of apatitic calcium phosphate is affected by other in-vivo conditions [39]. There are also studies that have reported different outcomes for the BSA presence with exactly the same experimental conditions [36,40]. Finally, there are studies that have reported positive effects of BSA presence on the osteogenic differentiation and growth of osteoblasts [38]. It is worth noting that only a few studies have clearly emphasized the role of protein type on the nucleation and growth of carbonated apatite [29,33]. Detailed investigations are necessary to be performed in the future to clarify the role of each protein contained in human blood plasma.

In contrast to all mentioned studies, the present work investigated the effects of physiological concentrations of the most abundant (95 % [47]) combination of human blood proteins HGG and HSA. HGG has been used as a model protein for different types of human globulins, which is a drawback. Nonetheless, taking into account the nominal composition of inorganic ions, buffering system, types, and concentrations of proteins, the protein-containing SBFs prepared in the present study mimicked the composition of the human blood very closely.

Table 4: Effects of proteins on the carbonated-forming-ability on the surfaces of various immersed model implants in various SBF formulations: present work vs. other related studies.

Ref/Year	Substrate(s)	Type of SBF	Buffering system	Type(s) and concentration(s) of protein(s)	Comments on the protein effects
[40] / 2001	Brushite layer on pure titanium	Ca^{2+}- and Mg^{2+}-free HBSS	TRIS	BSA / 1, 10, 30 g/L	Presence of BSA retards brushite to HA transformation
[36] / 2002	Brushite layer on a germanium crystal	Ca^{2+}- and Mg^{2+}-free HBSS	TRIS	BSA / 1, 10, 30 g/L	Presence of BSA does not affect the mechanism of brushite to HA transformation
[29] / 2004	HA, HA/α-TCP (86% HA + 14% α-TCP), and bioactive glass discs	Inorganic ion composition similar to r-SBF [18]	CO_2/HCO_3^- / regulated pH with continuous CO_2 bubbling	BSA / 4 g/L	BSA promotes the formation of apatitic calcium phosphate deposits
[37] / 2007	HA and fluorinated HA (FHA)	Kokubo's c-SBF with 4.2 mmol/ of HCO_3^-	TRIS-HCl	BSA / 40 g/L	BSA retards apatite precipitation from SBF onto the HA and FHA
[33] / 2012	HA	Inorganic ion composition similar to r-SBF [18]	HEPES-NaOH	BSA and LSZ (lysozyme) / 0.1, 1,10, 50 g/L	The growth rate of apatitic calcium phosphate was higher in the case of LSZ.
[41] / 2012	HA powder	Water	None	BSA and IgG (immunoglobulin G) / 1 g/L	BSA and IgG adsorb on the HA surface. IgG partially dissolves surface of HA particles upon mutual contact
[32] / 2017	Differently treated Ti-based discs	Kokubo's c-SBF with 4.2 mmol/ of HCO_3^-, BCS-1 and BCS-2 with inorganic ion composition similar to r-SBF [18]	TRIS-HCl for c-SBF and CO_2/HCO_3^- for BCS-1 and BCS-2 under 5% CO_2 atmosphere	BSA / 0.1, 1, 5 g/L	BSA has an inhibitory effect on nucleation of apatitic calcium phosphate on the surfaces of Ti-based discs in all SBFs. The effect is significantly stronger in the case of c-SBF
[38] / 2017	BCP discs (60% HA / 40% ß-TCP)	Kokubo's c-SBF with 4.2 mmol/ of HCO_3^-	TRIS-HCl + incubation in under 5% CO_2 atmosphere (CO_2/HCO_3^-)	BSA / 7 g/L	Positive effects on the osteogenic differentiation of osteoblasts. BSA enhanced cell growth significantly
[39] / 2017	Silica aerogel-based composites	Inorganic ion composition similar to r-SBF [18]	TRIS-HCl	BSA / 40 g/L + amino acids	BSA and amino acids do not produce any significant effect
Present work / 2021	Plasma-sprayed HACs	Inorganic ion composition similar to r-SBF [18]	Unregulated pH	HGG+HSA / 33 g/L + 44 g/L	HGG+HSA inhibits carbonated-apatite formation on the surface of plasma-sprayed HACs
Present work / 2021	Plasma-sprayed HACs	Inorganic ion composition similar to r-SBF [18]	CO_2/HCO_3^- / regulated pH with discontinuous CO_2 bubbling	HGG+HSA / 33 g/L + 44 g/L	HGG+HSA indifferently or positively affect the carbonated-apatite formation on the surfaces of plasma-sprayed HACs

The present work confirmed the bioactivity of the surfaces of plasma-sprayed HACs in the prepared protein-free and protein-containing SBFs. However, the opposite effects of protein presence on the carbonated-forming-ability have been confirmed in conditions of unregulated and regulated pH (Table 4). Here it should

be noted that the degree of supersaturation towards the carbonated apatite was very much different when the pH of SBF was unregulated and higher than in the case when it was regulated at 7.4±0.2 [23]. Therefore, in the present study, the protein effects on the carbonated-forming-ability may have been different under the

different experimental conditions (unregulated or regulated pH).

Strengths and shortcomings of the prepared SBFs coupled with the system for active pH regulation using CO_2

There are advantages of using the prepared SBFs and the system for active pH regulation using CO_2 [31] over the existing solutions [22,27-30,32]. A discontinuous CO_2 addition into the SBF and CO_2 release from the SBF into the ambient air resembles the mammalian respiratory function, whereas the dissolution of $NaHCO_3$ and $KHCO_3$ simulates the mammalian renal function. The system for active pH regulation using CO_2 does not require the items for CO_2 flow control or a sealed atmosphere with higher CO_2 partial pressure because it is designed to be a naturally open system. The conditions for conducting the experiments in a wide pH range (6.0-11.0) are established by an easy pH regulation utilizing a discontinuous CO_2 addition into the SBF. The initial SBF with high pH of 10.5±0.3 prepared in the present study can be stored for a long-term period because it does not contain Ca^{2+} ions. Long storage times can be achieved by decreasing the high pH of the initial SBF to 6.0 using CO_2 and by applying the proper hermetic sealing of the container containing such initial SBF. The use of the developed SBFs and system for active pH regulation with CO_2 has its own set of drawbacks. When the chemical interactions in the SBF create an acidic effect, the system for active pH regulation with CO_2 is unable to regulate the SBF pH adequately. The evaporation of water during long-term immersion testing of model implants cannot be avoided because the system for active pH regulation with CO_2 is an open system. Prepared SBFs, like other systems, must be refreshed after some period of the immersion testing of model implants. There are numerous methods to optimize the combination of prepared SBFs and the system for active pH regulation with CO_2, which will be the subject of future research.

CONCLUSIONS

In the present study, we prepared the initial SBF with the nominal composition of the inorganic ions close to that of the human blood plasma and with high pH of 10.5±0.3. Such pH was reduced around the physiological range (7.2) by the simple addition of CO_2 (protein-free SBFs) or a CO_2/human protein combination (protein-containing SBFs).

After reaching the starting pH of 7.2, the pH of prepared SBFs increased with time and it was unregulated during the pH instability testing. The dissolution of the physiological concentration of HGG+HSA reduced the pH instability of prepared SBFs by 60% and the presence of dissolved Ca^{2+} ions by 15 %, whereas the immersion of the plasma-sprayed HACs had an insignificant impact.

In conditions with unregulated pH, the dissolution of Ca^{2+} ions strongly affected the chemical instability of the protein-free SBFs, regardless of HACs presence. After 0.6-1-0 h, the protein-free SBFs became cloudy which indicated the onset of homogeneous precipitation of carbonated apatite. In conditions with regulated pH, protein-free SBFs remained transparent during the entire period of the HACs immersion testing. The chemical instability of protein-containing SBFs could not be visually confirmed due to their opacity.

The bioactivity of plasma-sprayed HACs was validated in the present study regardless of the experimental conditions (unregulated or regulated pH) or protein presence. FT-IR detected the formation of carbonated apatite on the surfaces of immersed HACs in protein-free SBFs and the simultaneous adsorption of proteins and formation of carbonated apatite in protein-containing SBFs. The dissolved HGG+HSA proteins inhibited the carbonated apatite forming on the surfaces of immersed HACs in conditions with unregulated pH. This effect was either neutral or beneficial in conditions of regulated pH.

REFERENCES

[1] Cuneyt T.A., The Use of Physiological Solutions or Media in Calcium Phosphate Synthesis and Processing, *Acta Biomaterialia*, **10**: 1771–1792 (2014).

[2] Ringer S., Concerning the Influence Exerted by Each of the Constituents of the Blood on the Contraction of the Ventricle, *J. Physiol.*, **3**: 380-393 (1882).

[3] Ringer S., A Further Contribution Regarding the Influence of the Different Constituents of the Blood on the Contraction of the Heart, *J. Physiol.*, **4**: 29-42 (1883).

[4] Ringer S., A Third Contribution Regarding the Influence of the Inorganic Constituents of the Blood on the Ventricular Contraction, *J. Physiol.*, **4**: 222–225 (1883).

[5] Durward A., Murdoch I., Understanding Acid-Base Balance, *Curr. Pediatr.*, **13**: 513-519 (2003).

[6] Matousek S., Handy J., Rees S.E., Acid-Base Chemistry of Plasma: Consolidation of Traditional and Modern Approaches from a Mathematical and Clinical Perspective, *J. Clin. Monit. Comp.*, **25**: 57–70 (2011).

[7] Jalota S., Bhaduri S.B., Tas A.C., Effect of Carbonate Content and Buffer Type on Calcium Phosphate Formation in SBF Solutions, *J. Mater. Sci: Mater. Med.*, **17**: 697–707 (2006).

[8] Kokubo T., Takadama H., How Useful is SBF in Predicting in Vivo Bone Bioactivity, *Biomaterials*, **27**: 2907–2915 (2006).

[9] Krebs H.A., Henseleit K., Untersuchungen ueber die Harnstoffbildung im Tierkoerper, *Hoppe-Seylers Z. Physiol. Chem.*, **210**: 33–66 (1932).

[10] Earle W.R., Production of Malignancy in Vitro. IV. the Mouse Fibroblast Cultures and Changes Seen in the Living Cells, *J. Nat. Cancer. Inst.*, **4**: 165–212 (1943).

[11] Hanks J.H., Wallace R.E., Relation of Oxygen and Temperature in the Preservation of Tissues by Refrigeration, *Proc. Soc. Exp. Biol. Med.*, **71**: 196–200 (1949).

[12] Hanks J.H., The Longevity of Chick Tissue Cultures without Renewal of Medium, *J. Cell. Comp. Physiol.*, **31**: 235–60 (1948).

[13] Kokubo T., Surface Chemistry of Bioactive Glass-Ceramics, *J. Non-Cryst.. Solids.*, **120**:138-151 (1990).

[14] Kokubo T., Bioactive Glass Ceramics: Properties and Applications, *Biomaterials*, **12**:155–163 (1991).

[15] Bayraktar D., Tas A.C., Chemical Preparation of Carbonated Calcium Hydroxyapatite Powders at 37°C in Urea-Containing Synthetic Body Fluids, *J. Eur. Ceram. Soc.*, **19**: 2573-2579 (1999).

[16] Tas A.C., Synthesis of Biomimetic Ca-hydroxyapatite Powders at 37°C in Synthetic Body Fluids, *Biomaterials*, **21**: 1429-1438 (2000).

[17] Bigi A., Boanini E., Panzavolta S., Roveri N., Biomimetic Growth of Hydroxyapatite on Gelatin Films Doped with Sodium Polyacrylate, *Biomacromolecules*, **1**: 752-756 (2000).

[18] Oyane A., Kim H.M., Furuya T., Kokubo T., Miyazaki T., Nakamura T., Preparation and Assessment of Revised Simulated Body Fluids, *J. Biomed. Mater. Res.*, **65(A)**: 188–195 (2003).

[19] Oyane A., Onuma K., Ito A., Kim H.M., Kokubo T., Nakamura T., Formation and Growth of Clusters in Conventional and New Kinds of Simulated Body Fluids, *J. Biomed. Mater. Res.*, **64(A)**: 339–348 (2003).

[20] Takadama H., Hashimoto M., Mizuno M., Kokubo T., Round-Robin Test of SBF for in Vitro Measurement of Apatite-Forming Ability of Synthetic Materials, *Phos. Res. Bull.*, **17**:119–125 (2004).

[21] Bohner M., Lemaitre J., Can Bioactivity be Tested in Vitro with SBF Solution?, *Biomaterials*, **30**: 2175–2179 (2009).

[22] Dorozhkina E.I., Dorozhkin S.V., Surface Mineralisation of Hydroxyapatite in Modified Simulated Body Fluid (mSBF) with Higher Amounts of Hydrogencarbonate Ions, *Colloid. Surf. A-Physicochem. Eng. Asp.*, **210**: 41–48 (2002).

[23] Muller L., Muller F.A., Preparation of SBF with Different HCO3- Content and its Influence on the Composition of Biomimetic Apatites, *Acta Biomater.*, **2**:181–189 (2006).

[24] Qu H., Wei M., The Effect of Temperature and Initial pH on Biomimetic Apatite Coating, *J. Biomed. Mater. Res. Part B: Appl. Biomater.*, **87(B)**: 204–212 (2008).

[25] Barrere F., van Blitterswijk C.A, de Groot K., Layrolle P., Influence of Ionic Strength and Carbonate on the Ca-P Coating Formation from SBF×5 Solution, *Biomaterials*, **23**: 1921–1930 (2002).

[26] Bachra B.N., Trautz O.R., Simon S.L., Precipitation of Calcium Carbonates and Phosphates. III. The Effect of Magnesium and Fluoride Ions on the Spontaneous Precipitation of Calcium Carbonates and Phosphates, *Arch. Oral. Biol.*, **10**: 731–738 (1965).

[27] Kim H.M., Kishimoto K., Miyaji F., Kokubo T., Composition and Structure of Apatite Formed on Organic Polymer in Simulated Body Fluid with a High Content of Carbonate Ion, *J. Mater. Sci: Mater. Med.*, **11**: 421-426 (2000).

[28] Marques P.A.A.P., Magalh M.C.F., Correia R.N., Inorganic Plasma with Physiological CO_2/HCO_3^- Buffer, *Biomaterials*, **24**:1541–1548 (2003).

[29] Marques P.A.A.P., Cachinho S.C.P., Magalhaes M.C.F., Correia R.N., Fernandes M.H.V., Mineralisation of Bioceramics in Simulated Plasma with Physiological CO_2/HCO_3^- Buffer and Albumin, *J. Mater. Chem.*, **14**: 1861–1866 (2004).

[30] Cai Q., Xu Q., Feng Q., Cao X., Yang X., Deng X., Biomineralization of Electrospun Poly(l-lactic acid)/ Gelatin Composite Fibrous Scaffold by Using a Supersaturated Simulated Body Fluid with Continuous CO_2 Bubbling, *Appl. Surf. Sci.*, **257**: 10109-10118 (2011).

[31] Schinhammer M., Hofstetter J., Wegmann C., Moszner F., Löffler J.F., Uggowitzer P.J., On the Immersion Testing of Degradable Implant Materials in Simulated Body Fluid: Active pH Regulation Using CO_2, *Adv. Eng. Mater.*, **15**:434–441 (2013).

[32] Zhao W., Lemaître J., Bowen P., A Comparative Study of Simulated Body Fluids in the Presence of Proteins, *Acta Biomater.*, **53**:506–514 (2017).

[33] Wang K., Leng Y., Lu X., Ren F., Ge X., Ding Y., Theoretical Analysis of Protein Effects on Calcium Phosphate Precipitation in Simulated Body Fluid, *Cryst. Eng. Comm.*, **14**: 5870–5878 (2012).

[34] Gross G., Moll W., Facilitated Diffusion of CO_2 Across Albumin Solutions, *J. Gen. Physiol.*, **64**:356-371 (1974).

[35] Chakraborty J., Chatterjee S., Sinha M.K., Basu D., Effect of Albumin on the Growth Characteristics of Hydroxyapatite Coatings on Alumina Substrates, *J. Am. Ceram. Soc.*, **90**:3360–3363 (2007).

[36] Xie J., Riley C., Kumar M., Chittur K., FTIR/ATR Study of Protein Adsorption and Brushite Transformation to Hydroxyapatite, *Biomaterials*, **23**: 3609–3616 (2002).

[37] Wang Y., Zhang S., Zeng X., Cheng K., Qian M., Weng W., In Vitro Behavior of Fluoridated Hydroxyapatite Coatings in Organic-Containing Simulated Body Fluid, *Mater. Sci. Eng. C*, **27**: 244–250 (2007).

[38] Huang L., Zhou B., Wu H., Zheng L., Zhao J., Effect of Apatite Formation of Biphasic Calcium Phosphate Ceramic (BCP) on Osteoblastogenesis Using Simulated Body Fluid (SBF) with or Without Bovine Serum Albumin (BSA), *Mater. Sci. Eng. C*, **70(C)**: 955–961 (2017).

[39] Gyori E., Fábián I., Lázár I., Effect of the Chemical Composition of Simulated Body Fluids on Aerogel-Based Bioactive Composites, *J. Compos. Sci.*, **1(2)**: 15 (2017).

[40] Xie J., Riley C., Chittur K., Effect of Albumin on Brushite Transformation to Hydroxyapatite, *J. Biomed. Mater. Res.*, **57**: 357–365 (2001).

[41] Pylypchuk E.V., Mishchenko V.N., Gromovoy T.Y., Interaction of Albumin and Immunoglobulin G with Synthetic Hydroxyapatite, *Chem. J. Mold.*, **7(2)**: 143-146 (2012).

[42] Vilotijević M., Marković P., Zec S., Marinković S., Jokanović V., Hydroxyapatite Coatings Prepared by a High Power Laminar Plasma Jet, *J. Mater. Process. Tech.*, **211**: 996–1004 (2011).

[43] Gligorijević B.R., Vilotijević M., Šćepanović M., Vuković N.S., Radović N.A., Substrate Preheating and Structural Properties of Power Plasma Sprayed Hydroxyapatite Coatings, *Ceram. Int.*, **42**: 411–420 (2016).

[44] Gligorijević B.R., Vilotijević M., Šćepanović M., Vidović D., Radović N.A., Surface Structural Heterogeneity of High Power Plasma-Sprayed Hydroxyapatite Coatings, *J. Alloys Compd.*, **687**: 421-430 (2016).

[45] Schneider C.A., Rasband W.S., Eliceiri K.W., NIH Image to Image J: 25 Years of Image Analysis, *Nat. Methods*, **9(7)**: 671-675 (2012).

[46] Garand E., Wende T., Goebbert D.J., Bergmann R., Meijer G., Neumark D.M., Asmis K.R., Infrared Spectroscopy of Hydrated Bicarbonate Anion Clusters: $HCO_3^-(H_2O)_{1-10}$, *J. Am. Chem. Soc.*, **132**: 849–85 (2010).

[47] Chambers D., Huang C., Matthews G., "Basic Physiology for Anaesthetists", Cambridge University Press, Cambridge, United Kingdom (2015).

[48] Bauer N., Panak P.J., Influence of Carbonate on the Complexation of Cm(III) with Human Serum Transferrin Studied by Time-Resolved Laser Fluorescence Spectroscopy (TRLFS), *New J. Chem.*, **39**:1375-1381 (2015).

[49] Pietrzyńska M., Voelkel A., Stability of Simulated Body Fluids Such as Blood Plasma, Artificial Urine and Artificial Saliva, *Microchem. J.*, **134**: 197–201 (2017).

[50] Curvale R.A., Buffer Capacity of Bovine Serum Albumin, *J. Argent. Chem. Soc.*, **97(1)**: 174-180 (2009).

[51] Lu X., Leng Y., Theoretical Analysis of Calcium Phosphate Precipitation in Simulated Body Fluid, *Biomaterials*, **26**: 1097–1108 (2005).

[52] Dridi A., Riahi K.Z., Somrani S., Mechanism of Apatite Formation on a Poorly Crystallized Calcium Phosphate in a Simulated Body Fluid (SBF) at 37 °C, *J. Phys. Chem. Solids*, **156**: 110-122 (2021).

[53] Du L.-W., Bian S., Gou B.-D., Jiang Y., Huang J., Gao Y.-X., Zhao Y.-D., Wen W., Zhang T.-L., Wang K., Structure of Clusters and Formation of Amorphous Calcium Phosphate and Hydroxyapatite: From the Perspective of Coordination Chemistry, *Cryst. Growth Des.*, **13**: 3103−3109 (2013).

[54] Sun L., Berndt C.C., Grey C.P., Phase, Structural and Microstructural Investigations of Plasma Sprayed Hydroxyapatite Coatings, *Mater. Sci. Eng. A*, **360**: 70-84 (2003).

[55] Hesse C., Hengst M., Kleeberg R., Gotze J., Influence of Experimental Parameters on Spatial Phase Distribution in As-Sprayed and Incubated Hydroxyapatite Coatings, *J. Mater. Sci. Mater. Med.*, **19**: 3235-3241 (2008).

[56] Zhang Q., Chen J., Feng J., Caoa Y., Deng C., Zhang X., Dissolution and Mineralization Behaviors of HA Coatings, *Biomaterials*, **24**:4741–4748 (2003).

[57] Fleet M.E., Infrared spectra of carbonate apatites: υ2-Region Bands, *Biomaterials*, **30**: 1473–1481 (2009).

[58] Luong L.N., Hong S.I., Patel R.J., Outslay M.E., Kohn D.H., Spatial Control of Protein within Biomimetically Nucleated Mineral, *Biomaterials*, **27**: 1175–1186 (2006).

[59] Kragh-Hansen U., Vorum H., Quantitative Analyses of the Interaction between Calcium Ions and Human Serum Albumin, *Clin. Chem.*, **39**: 202-208 (1993).

[60] Fogh-Andersen N., Bjerrum P.J., Siggaard-Andersen O., Ionic Binding, Net Charge, and Donnan Effect of Human Serum Albumin as a Function of pH, *Clin. Chem.*, **39**: 48-52 (1993).